

EFFECT OF A NANO-SCALE FINE HOLE PATTERN ON THE DIFFERENTIATION OF RAW264.7 CELLS INTO OSTEOCLASTS

R. TAKATA^a, T. AKASAKA^{b*}, M. TAMAI^b, Y. YOSHIMURA^c, T. TAIRA^d,
H. MIYAJI^e, Y. TAGAWA^f, S. YAMAGATA^a, J. IIDA^a, Y. YOSHIDA^b

^a*Department of Orthodontics, Faculty of Dental Medicine and Graduate School of Dental Medicine, Hokkaido University, Sapporo 060-8586, Japan*

^b*Department of Biomaterials and Bioengineering, Faculty of Dental Medicine, Hokkaido University, Sapporo 060-8586, Japan*

^c*Department of Molecular Cell Pharmacology, Faculty of Dental Medicine and Graduate School of Dental Medicine, Hokkaido University, Kita-ku, Sapporo 060-8586, Japan*

^d*Cosmo Bio Co., Ltd., Sapporo Division, 3-513-2, Zenibako, Otaru Hokkaido 047-0261, Japan*

^e*Department of Periodontology and Endodontology, Faculty of Dental Medicine, Hokkaido University, Sapporo 060-8586, Japan*

^f*School of Life Science and Technology, Tokyo Institute of Technology, 4259 B51, Nagatsuta-cho, Midori-ku, Yokohama, Kanagawa 226-8501, Japan*

Osteoclasts are associated with certain diseases such as osteopetrosis. The development and functions of osteoclasts are controlled by the micro- and nano-surface roughness of biomaterials. However, the effect of fine micro/nano-patterns on osteoclastic differentiation remains poorly understood. In the present study, we investigated the effect of fine shape patterns at the nano-scale on osteoclastic differentiation. A hole pattern of 500 nm in diameter and 500 nm in height was prepared using nanoimprinting of a glycol-modified polyethylene terephthalate (G-PET) film for a basic topological study. RAW264.7 cells were used as an alternative basic model to primary cells. The result of a cell attachment assay showed that the average number of attached cells on the hole patterned-film was 1.5 times higher than that on the planar film. A cell differentiation assay showed that the average number of multinucleated osteoclasts on the hole patterned-film was approximately 1.9 times higher than that on the planar film. However, the patterning effects in this study were quite small ($p > 0.05$). Although the morphology of the cells was basically similar when observed under an optical microscope, the morphologies of the attached and differentiated cells were slightly different in terms of their cell shape and filopodia shape between the holed and planar films when observed under a scanning electron microscope. Differences in cell attachment and differentiation behaviors between holed and planar films would affect the functions of the osteoclasts. We suggest that fine nano-patterning of the substrate could be one factor to control osteoclastic differentiation and cell function.

(Received January 31, 2018; Accepted April 26, 2018)

Keywords: Cell attachment; Differentiation; Nano-pattern; Hole pattern; RAW264.7 cells; Osteoclasts

*Corresponding author: akasaka@den.hokudai.ac.jp

1. Introduction

Bone tissue is continuously remodeled by the balanced activities between resorption of bone by osteoclasts and formation of new bone by osteoblasts. Osteoclasts are derived from osteoclast precursor cells, including monocytes and macrophages [1]. Mature osteoclasts are large multinucleated cells formed by cell fusion and have bone resorption activity [2]. Furthermore, osteoclasts are associated with certain diseases, such as osteopetrosis, osteoporosis, osteolysis, inflammatory arthritis, and Paget's disease of bone [3].

The development and functions of osteoclasts are affected by the micro- and nano-surface roughness of biomaterials. Marchisio et al. reported that titanium with a rougher surface was a more effective material surface for the differentiation of RAW264.7 macrophage cells into osteoclasts than smooth titanium [4]. Davison et al. reported that osteoclasts grown on a calcium phosphate disk with submicro-scaled surface architecture were larger and more active than osteoclasts grown on a calcium phosphate disk with micro-scaled surface architecture [5]. Park et al. reported that the number of multinucleated osteoclasts differentiated from hematopoietic stem cells on 15 nm titanium nanotubes was the highest among different pore sizes of titanium nanotubes with diameters of 15 to 100 nm [6]. These data indicated that the development and functions of osteoclasts were sensitive to topological factors. Thus, the effect of fine shape structures at the micro/nano-scale on osteoclastic differentiation should be investigated.

In the only previous study about osteoclastic differentiation on fine shape structures, Niida et al. reported that osteoclasts differentiated from osteoclast precursor cells on titan-coated micro-grooves [7]. The osteoclasts could be well orientated along the direction of grooves with a width of 1 μm . However, the efficiency of differentiation on fine patterns at the micro/nano-scale has not been investigated and their effect on osteoclastic differentiation remains poorly understood.

Surface micro/nano-patterns of biomaterials significantly affect cell adhesion, spreading, morphology, proliferation, and differentiation [8,9]. Our previous reports described the development of fine micro/nano-patterns that employ an apatite paste [10], a titanium coat [11], a flowable composite resin [12], and curable dental materials [13]. The behavior of osteoblastic cells and fibroblastic cells on surfaces with fine patterns can be altered by designing different materials and surface patterns.

In the present study, we investigated the effect of fine shape pattern at the nano-scale on osteoclastic differentiation. A hole pattern with a diameter of 500 nm and a height of 500 nm was prepared by nanoimprinting of a glycol-modified polyethylene terephthalate (G-PET) film as a basic topological study. To estimate the cell attachment and differentiation behaviors on the patterned film, RAW264.7 cells were used as an alternative basic model to primary cells. The murine RAW264.7 pre-osteoclast cell line is a useful cell system because they can be differentiated into osteoclasts by the addition of the receptor activator of NF- κ B ligand (RANKL).

2. Materials and Methods

2.1. Preparation of the G-PET patterned film

The G-PET hole pattern was prepared according to a previously reported method [12]. The quartz master mold was purchased from Kyodo International, Inc. (Kawasaki, Japan). The area of $5 \times 5 \text{ mm}^2$ used in this study was patterned with pillars of 500 nm in diameter and 500 nm high. Replicas of the master mold were prepared by heat-pressing on a G-PET film (Sawada Platic Co., Ltd., Saitama, Japan) with the master mold using a compact heating press (AH-1TC, ASONE Co., Osaka, Japan) at 105°C for 4 min under a pressure of 2 MPa. The resulting G-PET hole-patterned film was carefully peeled off from the mold. Before the cell attachment and differentiation assays, the patterned film was fixed on a 3.5-cm or 6-cm tissue culture dish (AGC Techno Glass Co., Ltd., Shizuoka, Japan) and sterilized under UV irradiation for 6 min. To observe the surface of pattern [12], the film was coated with Pt-Pd using a sputtering apparatus (E-1030; Hitachi High-Tech

Fielding Co., Tokyo, Japan). The surface morphology of the patterned film was observed using scanning electron microscopy (SEM; S-4000; Hitachi High-Tech Fielding Co.).

2.2. Cell attachment assay

To estimate cell attachment on the patterned film, we carried out a cell attachment assay using the murine monocyte/macrophage cell line RAW264.7 (ATCC no. TIB-71TM, USA), as previously reported [12, 14]. The cells were grown to subconfluence in 10-cm tissue culture dishes (AGC Techno Glass Co., Ltd.) in Dulbecco's modified Eagle's medium (DMEM; Sigma-Aldrich, St. Louis, MO, USA) containing 10% fetal bovine serum (FBS; CELLelect™ Silver; MP Biomedicals, Santa Ana, CA, USA) and 1% penicillin-streptomycin-amphotericin B suspension (Wako Pure Chemical Industries, Ltd., Osaka, Japan) at 37°C in a humidified 5% CO₂/95% air atmosphere. Subsequently, the cells were collected by scraping and seeded at a density of 76,000 cells/cm² on the hole-patterned-film fixed in 6-cm tissue culture dishes. The cells were incubated with DMEM containing 10% FBS and 1% penicillin-streptomycin-amphotericin B suspension at 37°C in a humidified 5% CO₂/95% air atmosphere for 1 hour. The number of the attached cells was then determined by optical microscope observation after Giemsa staining [12]. The patterned film was rinsed with phosphate-buffered saline (PBS) to remove the non-adhering cells, fixed with a solution of 2.5% glutaraldehyde, and stained with Giemsa dye. The numbers of the attached cells were counted from six different random fields of 3.55 mm²/field for each patterned film from the optical microscope images. Values represent the mean and standard deviation of four experiments.

2.3. Cell differentiation assay

To estimate cell differentiation on the patterned film, we carried out an osteoclastic differentiation assay using RAW264.7 cells as osteoclast precursors, as previously reported [15]. The stored RAW264.7 cells were pre-cultured for 1 day. The cells were collected by scraping and seeded at a density of 5,000 cells/cm² on the hole-patterned films fixed in 3.5-cm tissue culture dishes. The cells were cultured with α -minimum essential medium (α -MEM; Gibco, Grand Island, NY, USA) containing 10% FBS, 1% penicillin-streptomycin-amphotericin B suspension, and 200 ng/ml recombinant soluble RANKL (sRANKL; Oriental Yeast Co., Ltd., Tokyo, Japan) at 37°C in a humidified 5% CO₂/95% air atmosphere for 6 days. The culture medium was changed every 2 days. To confirm osteoclastic differentiation, the cells were assessed by cytochemical staining for tartrate-resistant acid phosphatase (TRAP) [15,16]. The cells cultured after 6 days were washed with PBS and fixed with 4% paraformaldehyde (Wako Pure Chemical Industries, Ltd) for 5 min. Subsequently, the cells were washed with distilled water by pipetting and stained using a TRAP staining kit (Cosmo Bio Co., Ltd., Tokyo, Japan) according to manufactures instructions. The numbers of osteoclasts were counted from six different random fields of 2.23 mm²/field for each patterned film from the optical microscope images. TRAP-positive osteoclasts with >3 nuclei were counted as multinucleated osteoclasts. Values represent the mean and standard deviation of four experiments.

2.4. SEM observation of the cells

For SEM observation of the cells [12], the cells on the patterned films were rinsed with PBS, fixed with a solution of 2.5% glutaraldehyde, and then dehydrated in a graded series of alcohol (50%, 60%, 70%, 80%, 90%, 95%, 99.5%, and 100%) followed by drying in liquefied carbon dioxide at 25°C for a short time (approximately 3 min). The typical critical-point drying procedure was not carried out because the G-PET film is chemically weak during long-term exposure in liquefied carbon dioxide. The dried cells on the patterned were coated by Pt-Pd sputtering. The morphology of the cells was then observed using SEM.

2.5. Statistical analysis

Statistical analysis was performed using GraphPad Prism version 6.04 (GraphPad Software, Inc., La Jolla, CA, USA). All data are presented as the mean \pm standard deviation. Statistical differences were assessed using an unpaired t test. A value of $p < 0.05$ was considered

statistically significant.

3. Results and discussion

3.1. Preparation of the G-PET hole patterned film

Figure 1a shows the procedure for patterning of the G-PET films via thermal nanoimprinting. The advantage of the G-PET film for thermal nanoimprinting is that it is easily transferred because of its lower glass transition temperature compared with that of typical PET films [17,12]. Furthermore, G-PET films are non-toxic and stable in a cell culture medium. The wettability of the surface of planar G-PET films indicates higher hydrophilic property than the surface of typical PET films. Thus, we selected G-PET films for the cell attachment and cell differentiation assays of RAW264.7 cells (Figure 1b) as a primary basic study.

The SEM images of the G-PET hole-patterned film transferred by the quartz mold with pillars of 500 nm in diameter and 500 nm high are shown in Fig. 2. The fine shape of the hole was observed as the corresponding fine shape of the pillar mold. The G-PET planar film was observed to have a smooth surface at the submicro level.

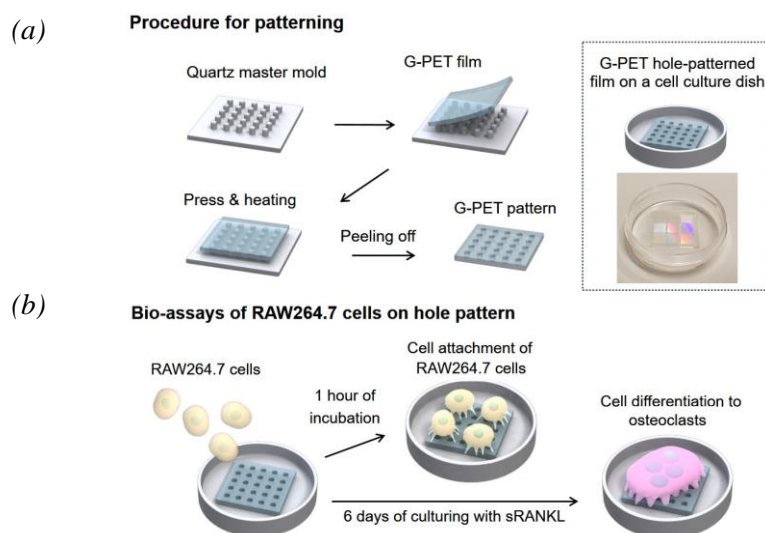
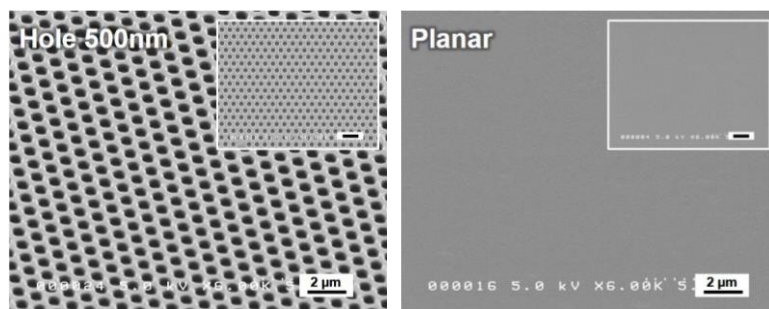


Fig. 1. Illustrations of (a) the procedure for patterning a poly(ethylene terephthalate)-glycol (G-PET) film by nanoimprinting; and (b) cell attachment and cell differentiation assays of RAW264.7 cells on hole-pattern films.



(a)

(b)

Fig. 2. SEM images of the surface of G-PET patterned film at a 45° tilt angle and a top view. (a) Hole pattern of 500 in nm diameter and 500 nm high, and (b) a planar film. The inset black scale bar represents 2 μm.

3.2. Cell attachment on the patterned film

Fig. 3a shows representative SEM images of RAW264.7 cells attached on G-PET patterned films after 1 hour of incubation. The morphology of the attached cells was different between the hole-patterned and planar films. The cells on the hole-patterned film exhibited a roughly round shape and were slightly extended, whereas the cells on the planar film were spread radially and had a flattened shape. The cells on the planar film were spread wider than those on the hole-patterned film. The wider spreading of the RAW264.7 cells on the G-PET planar surface was similar to that observed on a polystyrene planar film compared with a polystyrene nano-grooved film [18]. A difference in morphology was also observed for RAW264.7 cells cultured on different sizes of alumina nano-pores [19]. Fig. 3b shows the number of attached cells on G-PET patterned films after 1 hour of incubation. The average number of attached cells on the hole patterned was 1.5 times higher than that on the planar film. However, the difference was not significant ($p > 0.05$). Increasing attachment of RAW264.7 cells by patterning agreed with the previously observed increased attachment of mononuclear cells on the rougher surfaces of bone or dentin compared with smooth surfaces [20]. By contrast, a decreased attachment resulting from patterning was observed for chitosan copolymer nano-rods with diameters of 170 or 300 nm using RAW264.7 cells compared with the corresponding planar surfaces [21]. Thus, these differences in cell attachment behavior could depend on the size and shape of the patterns, and the surface chemical composition. At the early stage of cell attachment on the G-PET patterned films (1 hour of incubation), the hole pattern would induce cell attachment but prevent cell spreading according to the shape or roughness of the hole.

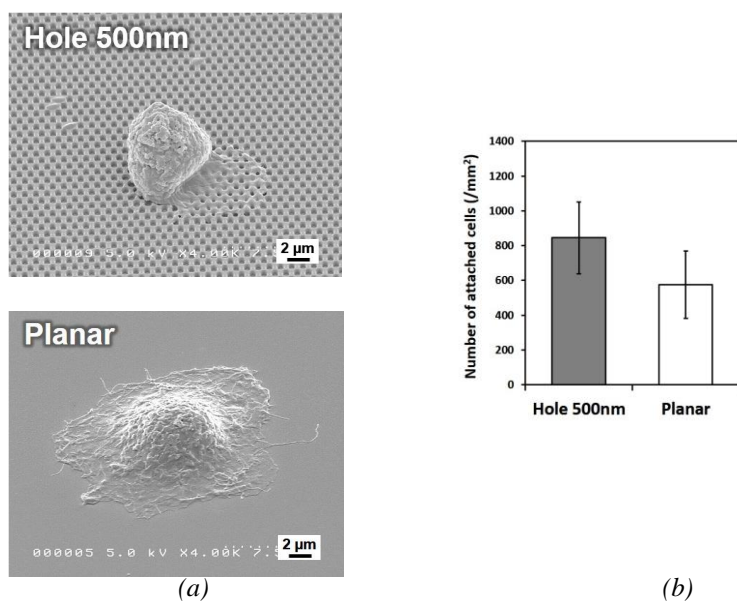


Fig. 3. Cell attachment assay of RAW264.7 cells to G-PET patterned films. (a) Representative SEM images of the attached cells on a hole patterned film with holes with a diameter of 500 nm diameter and a height of 500 nm or a planar film at a 45° tilt angle. (b) Bar graph of the number of attached cells on the hole-patterned film or the planar film after 1 hour of incubation. Data are the mean \pm standard deviation ($n = 4$). There was no statistical difference when analyzed by an unpaired t test ($p > 0.05$).

3.3. Cell differentiation of RAW264.7 into osteoclasts

Figure 4 shows the cell differentiation assay of RAW264.7 cells into mononuclear or multinucleated osteoclasts after 6 days of culture stimulated with sRANKL. Representative light microscope images of TRAP staining of the cells are shown in Fig. 4a. TRAP is an osteoclast marker enzyme. The red-stained cells are TRAP-positive cells, indicating differentiation of RAW264.7 cells into osteoclasts. Some TRAP-positive multinucleated cells, indicated by white arrows in Fig 4a, were observed on both hole-patterned and planar films. The morphology of the

cells was basically similar under optical microscope observation. Fig. 4b shows the number of multinucleated osteoblasts with >3 nuclei on the G-PET patterned films. The patterning of the G-PET film slightly affected the efficiency of differentiation of RAW264.7 cells into multinucleated osteoclasts. The average number of multinucleated osteoclasts on the hole-patterned film was approximately 1.9 times higher than that on the planar film. However, there was no significant difference ($p > 0.05$). Increasing numbers of osteoclasts on the patterned film agreed with the reported increased number of osteoclasts in response to titanium surfaces with increasing surface roughness [4,22,23]. Furthermore, Makihira et al. reported that surface roughing enhanced the mRNA expression levels of RANKL receptor, RANK, and its adaptor protein TNF receptor-associated factor 6 (TRAF6) of RAW264.7 cells cultured on titanium substrates [23]. Greater surface roughness of substrates would enhance surface wettability and protein adsorption, resulting in the induction of osteoclast development [24]. Therefore, our hole-patterning at the nano-level slightly activated RAW264.7 cells to differentiate into multinucleated osteoclasts. However, the patterning effect in this study was relatively small.

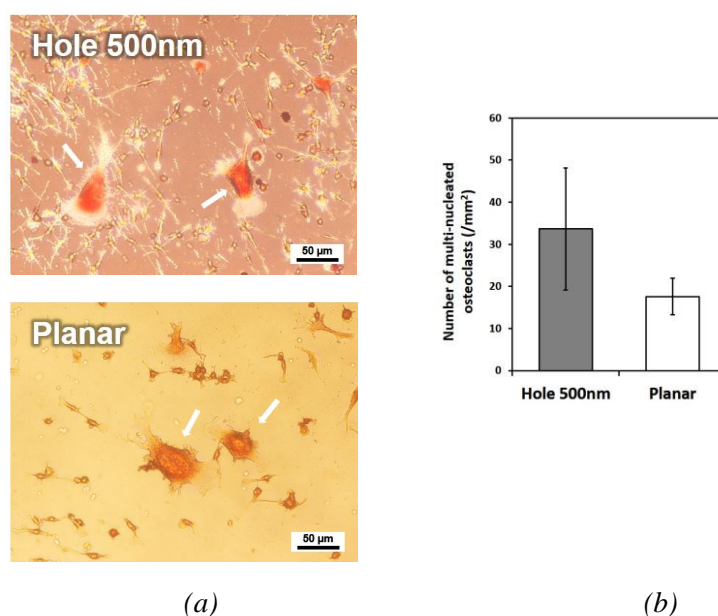


Fig. 4. Cell differentiation assay of RAW264.7 cells into osteoclasts on a G-PET hole-patterned film with holes with a diameter of 500 nm and a height of 500 nm or on a G-PET planar film. The cells were cultured for 6 days. (a) Representative light microscope images of tartrate resistant acid phosphatase (TRAP) staining of osteoclasts originated from RAW264.7 cells. TRAP activity was visualized by TRAP staining (Red). White arrows indicate multinucleated osteoclasts with >3 nuclei. (b) Bar graph of the number of multinucleated osteoclasts with >3 nuclei. Data are the mean \pm standard deviation ($n = 4$). There was no statistical difference when analyzed by an unpaired t test ($p > 0.05$).

Fig. 5 shows SEM images of the characteristic morphology of osteoclasts originating from RAW264.7 cells on G-PET patterned films after 6 days of culture. White arrows indicate multinucleated osteoclasts. Although many cells were observed as mononuclear cells, indicating RAW264.7 cells or mononuclear osteoclasts with a small area, a small number of the cells were observed as multinucleated cells with a large area. The multinucleated osteoclasts on both the holed and planar films were observed as various cell shapes and areas (part of the data are shown in Fig. 5). There was no large difference in cell shape and area between cells cultured on the holed and planar films. If anything, the multinucleated osteoclasts on hole-patterned film seem to be slightly smaller and more corner-shaped than the multinucleated osteoclasts on the planar film. The small area of osteoclasts on the hole-patterned film is similar to the small area of osteoclasts on a titanium rough surface [22]. Cell elongation of multinucleated osteoclasts might be slightly

disturbed by the hole shapes at the nano level. Interestingly, the filopodia of osteoclasts on the hole-patterned film seemed to attach to the edge of the hole shape. Thus, the strength of osteoclast attachment on hole-pattern film might be stronger because of grasping by the filopodia. Practically, osteoclasts on a planar film can be more easily detached by pipetting. Differences in cell attachment behavior and strength between holed and planar films would affect osteoclast functions.

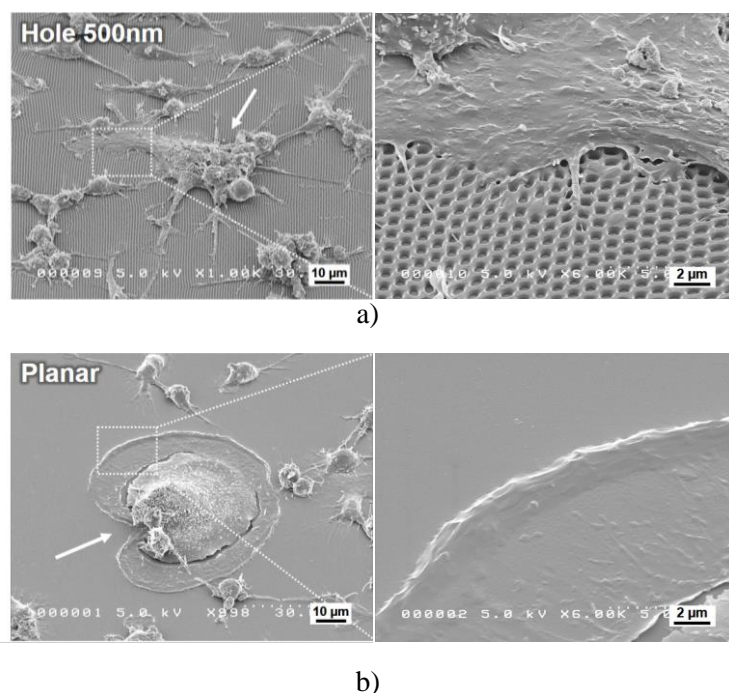


Fig. 5. Characteristic SEM images of osteoclasts originating from RAW264.7 cells after 6 days of culture. The cells were cultured on (a) a G-PET hole-patterned film with holes with a diameter of 500 nm and a height of 500 nm; and (b) a G-PET planar film as a control. The right images are at a higher magnification, and the left images are at lower magnification. White arrows indicate multinucleated osteoclasts.

4. Conclusions

We prepared a G-PET hole-pattern film at the nano level and estimated to influence of the pattern on cell attachment and osteoclastic differentiation of RAW264.7 cells as a basic study. Our results suggested that cell attachment and osteoclastic differentiation were slightly improved by hole patterning. However, the patterning effects in this study were relatively small ($p > 0.05$). Interestingly, the filopodia of osteoclasts on the hole patterned film appeared to grasp the edge of hole shape under SEM observation. Differences in cell attachment and differentiation behaviors between the holed and planar films would affect osteoclast functions. Our preliminary study supports the view that fine nano-patterning of a substrate would be one factors to control osteoclastic differentiation and cell functions. The ideal fine micro/nano patterns have not been identified yet. Further comparative studies of osteoclast differentiation on several different types of fine micro/nano-patterns are required.

Acknowledgments

This work was funded by JSPS KAKENHI Grant Number (JP25463047 and JP16K11822), Suzuken Memorial Foundation, and “Building of Consortia for the Development of Human

Resources in Science and Technology” through Ministry of Education, Culture, Sports, Science and Technology, Japan. We would like to thank Editage (www.editage.jp) for English language editing.

References

- [1] N. Takahashi, N. Udagawa, T. Suda, *Biochem. Biophys. Res. Commun.* **256**, 449 (1999).
- [2] R. Detsch, A. R. Boccaccini, *J. Tissue Eng. Regen. Med.* **9**, 1133 (2015).
- [3] D. V. Novack, S. L. Teitelbaum, *Annu. Rev. Pathol.* **3**, 457 (2008).
- [4] M. Marchisio, M. Di Carmine, R. Pagone, A. Piattelli, S. Miscia, *J. Biomed. Mater. Res.* **75B**, 251 (2005).
- [5] N. L. Davison, X. Luo, T. Schoenmaker, V. Everts, H. Yuan, F. Barrère-de Groot, J. D. de Bruijn, *Eur. Cell. Mater.* **27**, 281 (2014).
- [6] J. Park, S. Bauer, K. A. Schlegel, F. W. Neukam, K. von der Mark, P. Schmuki, *Small* **5**, 666 (2009).
- [7] A. Niida, Y. Abiko, T. Yui, Y. Hirose, M. Ochi, *J. Jpn. Soc. Oral Implant.* **26**, 651 (2013) (in Japanese).
- [8] M. Nikkhah, F. Edalat, S. Manoucheri, A. Khademhosseini, *Biomaterials* **33**, 5230 (2012).
- [9] M. J. P. Biggs, R. G. Richards, M. J. Dalby, *Nanomedicine* **6**, 619 (2010).
- [10] T. Akasaka, H. Miyaji, N. Kaga, A. Yokoyama, S. Abe, Y. Yoshida, *Nano Biomedicine* **8**, 112 (2016).
- [11] K. Kaga, T. Akasaka, R. Horiuchi, Y. Yoshida, A. Yokoyama, *Nano Biomedicine* **8**, 74 (2016).
- [12] T. Akasaka, T. Imamura, H. Miyaji, N. Kaga, A. Yokoyama, Y. Yoshida, *e-J. Surf. Sci. Nanotech.* **14**, 225 (2016).
- [13] T. Akasaka, H. Miyaji, T. Imamura, N. Kaga, A. Yokoyama, Y. Yoshida, *Dig. J. Nanomater. Bios.* **12**, 281 (2017).
- [14] T. Akasaka, S. Abe, F. Watari, *Key Eng. Mater.* **529-530**, 379 (2013).
- [15] K. Shibata, Y. Yoshimura, T. Kikuri, T. Hasegawa, Y. Taniguchi, Y. Deyama, K. Suzuki, J. Iida, *Int. J. Mol. Med.* **28**, 73 (2011).
- [16] A. Omori, Y. Yoshimura, Y. Deyama, K. Suzuki, *Biomed. Rep.* **3**, 483 (2015).
- [17] R. B. Dupaix, M. C. Boyce, *Polymer* **46**, 4827 (2005).
- [18] E. Lamers, X. F. Walboomers, M. Domanski, L. Prodanov, J. Melis, R. Luttge, L. Winnubst, J. M. Anderson, H. J. Gardeniers, J. A. Jansen, *Nanomedicine* **8**, 308 (2012).
- [19] S. Pujari, A. Hoess, J. Shen, A. Thormann, A. Heilmann, L. Tang, M. Karlsson-Ott, *J. Biomed. Mater. Res. A* **102**, 3773 (2014).
- [20] M. Rumpler, T. Würger, P. Roschger, E. Zwettler, I. Sturmlechner, P. Altmann, P. Fratzl, M. J. Rogers, K. Klaushofer, *Calcif. Tissue Int.* **93**, 526 (2013).
- [21] M. L. Lastra, M. S. Molinuevo, I. Blaszczyk-Lezak, C. Mijangos, M. S. Cortizo, *J. Biomed. Mater. Res. A* **106**, 570 (2018).
- [22] J. Brinkmann, T. Hefti, F. Schlottig, N.D. Spencer, H. Hall, *Biointerphases* **7**, 34 (2012).
- [23] S. Makihira, Y. Mine, E. Kosaka, H. Nikawa, *Dent. Mater. J.* **26**, 739 (2007).
- [24] T. J. Webster, C. Ergun, R. H. Doremus, R. W. Siegel, R. Bizios, *Biomaterials* **22**, 1327 (2001).